24 th. EUROPEAN ROTORCRAFT FORUM
Marseilles, France - 15th. - 17th. September 1998

REFERENCE : TE 01

DYNAMIC VALIDATION OF A STIFF-IN-PLANE BEARINGLESS TAIL ROTOR OF ADVANCED LIGHT HELICOPTER

K. S. Narayana Rao - B. Pranesh - N. K. Maiti
Rotary Wing Research & Design Centre
Hindustan Aeronautics Limited
Bangalore, India

A four bladed, stiff-in-plane, bearingless tail rotor is designed and developed for Advanced Light Helicopter (ALH). With the application of composite material in design of bearingless tail rotor, optimised dynamic characteristics with respect to frequencies, loads and aeroelastic stability were achieved. Extensive ground tests were conducted to prove the strength of the tail rotor components. The tail rotor was tested on a specially designed whirl tower for the performance, loads, frequencies and aeroelastic stability characteristics over the complete range of rotational speed, collective pitch angles and precession. Flight tests are conducted to check steady and dynamic loads occurring during different flight conditions such as level, climb, descents, sideward, sideslips and special manoeuvering flights. This paper gives an overview of design and development efforts for dynamic validation of the bearingless tail rotor.

1. INTRODUCTION

A four-bladed, stiff-in-plane, bearingless tail rotor has been designed and developed for Advanced Light Helicopter (ALH). It is a pusher type rotor.

A stiff-in-plane rotor is ideal from aeromechanical stability point of view even though it introduces higher inplane dynamic loads. Application of composite materials in blade design has made it possible to realise a dynamically tuned, stiff-in-plane, bearingless tail rotor.

A general description, dynamic characteristics, whirl tower test results and some of the flight test results pertaining to tail rotor are presented in this paper.

2. OBJECTIVES

The tail rotor of ALH has been designed and developed with the following objectives :

- simple in design with respect to geometry and part count
- good dynamic characteristics with low vibration levels
- good low-speed handling characteristics essential for operations in restricted zone such as ship decks
- better manoeuverability during forward and sideslip flights

3. GENERAL DESCRIPTION

The tail rotor blade of 2.55m dia. is composed of flexbeam, pitch case and airfoil profile portion (Fig. 1). A pair of blades are connected together with a single flexbeam and constructed as one unit.

The tail rotor hub consists of two metal plates between which the flexbeams of each blade pair are sandwiched (Fig. 2). Hub plates are attached to the shaft by splines so as to transmit the torque. The flexbeam is constructed using predominantly unidirectional glass/epoxy composite material which has low torsional stiffness. Torsional moments required for pitch articulation are transmitted through pitch case which is made of ±45° glass/epoxy layers thus ensuring required torsional rigidity. An elastomeric snubber bearing, acting as a shear restraint, is positioned between the pitch case and flex beam. The blade has a complex shape with cambered airfoil with linear twist distributions. The

airfoil portion of the blade has been designed to realise the required mass, stiffness, centre of gravity and elastic axis positions so as to result in low blade loads and vibrations. Erosion protection is provided through a nickel strip bonded to the leading edge.

Collective variation of tail rotor blade pitch angles is done by spider mechanism. The four-armed spider is rigidly connected to a control tube which is located inside the tail rotor shaft. The control tube slides inside the rotor shaft depending on tail rotor actuator inputs. Each spider arm is connected to pitch horn of the blade through an adjustable pitch link.

4. DYNAMIC LAYOUT

Placement of blade natural frequencies has a large influence on the stability, controllability and response characteristics of the tail rotor. To fulfil this, the mass and stiffness distribution along the blade have been optimised over the operating speed of the rotor such that the frequencies are well placed to avoid coalescence with the harmonics of rotor speed. In arriving at acceptable frequencies, several iterations were performed to estimate the uncoupled frequencies in flap, lead-lag and torsion by transfer matrix approach. The mass distribution along the radius of the blade is shown in Fig. 3.

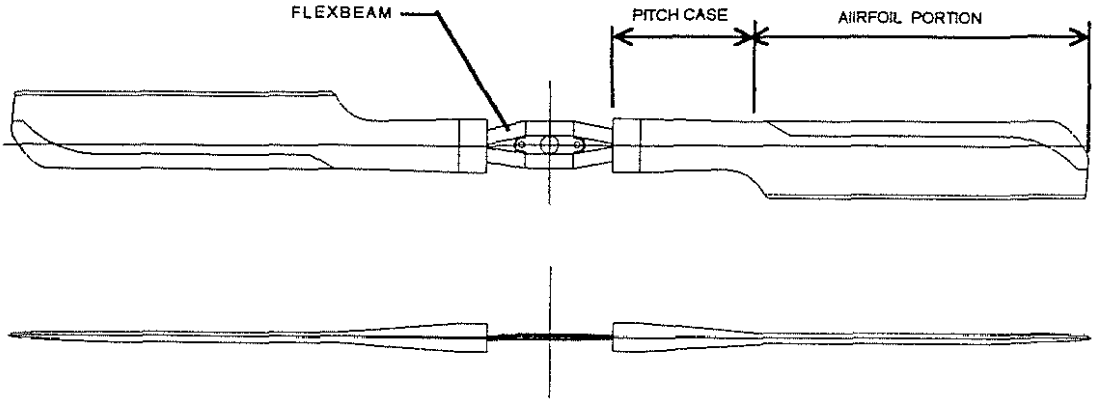

Fig. 1 : Tail Rotor Blade pair assembly

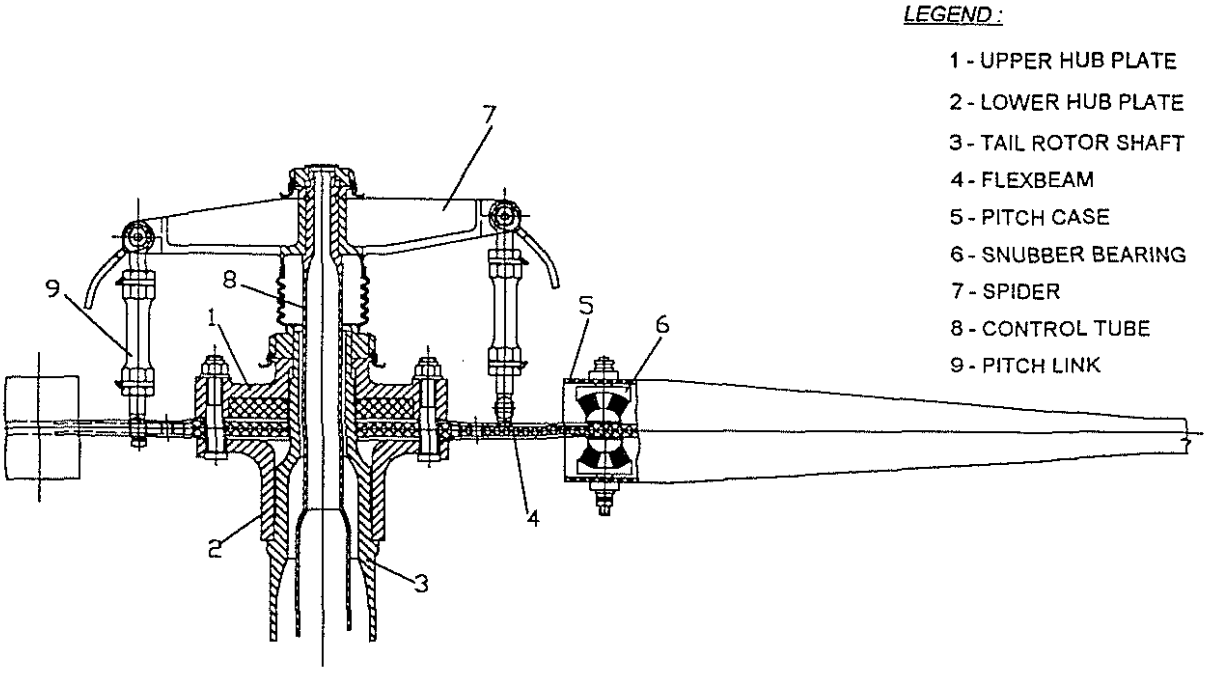

Fig. 2 : Tail Rotor Assembly

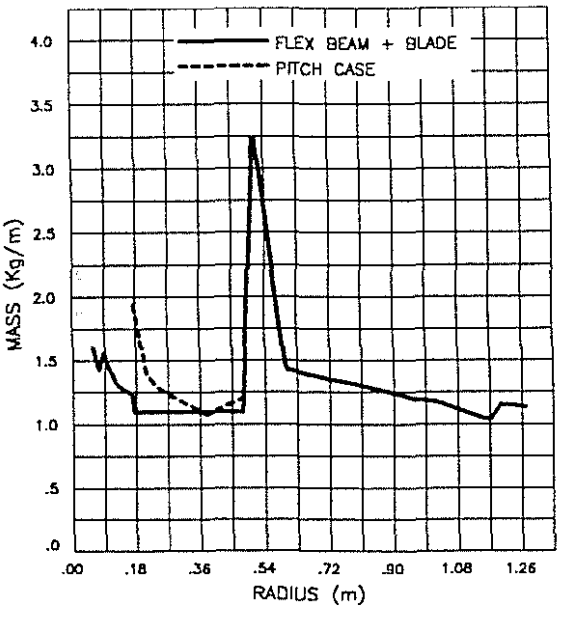

Fig. 3 : Mass distribution along radius of tail rotor blade

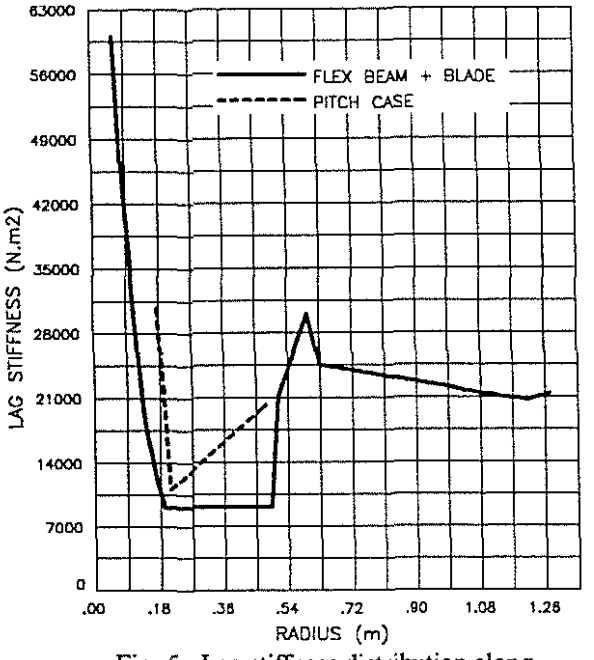

Fig. 5 : Lag stiffness distribution along the radius of tail rotor blade

The flexbeam, tapered in width and thickness at root, was carefully tailored to achieve an equivalent flap hinge offset of 11.5% so as to obtain required optimum hub loads and strain levels. The tailored flapwise bending stiffness distribution along the radius of the blade is shown in Fig. 4. The chordwise bending stiffness distribution along the radius of the blade is shown in Fig. 5.

The reduction in excessive blade flapping is achieved by using an equivalent δ_3-coupling provided by the location of the pitch horn. The fundamental flap and lead-lag frequencies are well separated considering δ_3 effects.

The torsional stiffness of the flexbeam has been optimised to minimise the control loads. The tailored torsional stiffness distribution along the radius of the blade is shown in Fig. 6.

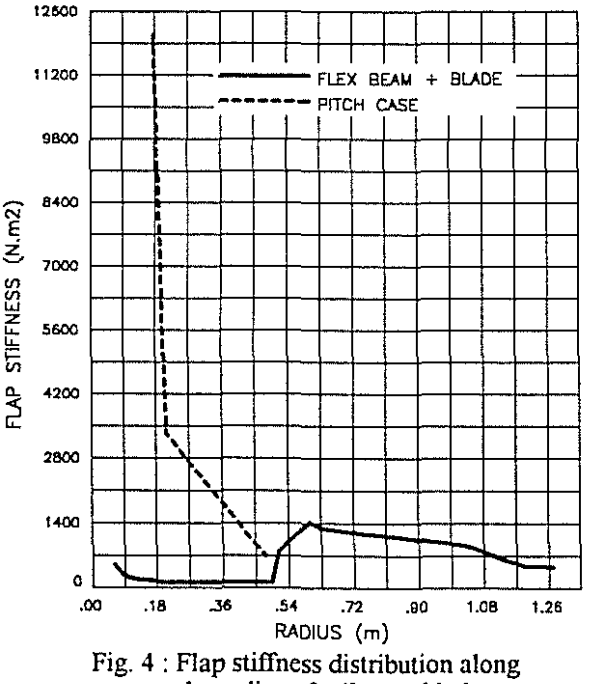

Fig. 4 : Flap stiffness distribution along the radius of tail rotor blade

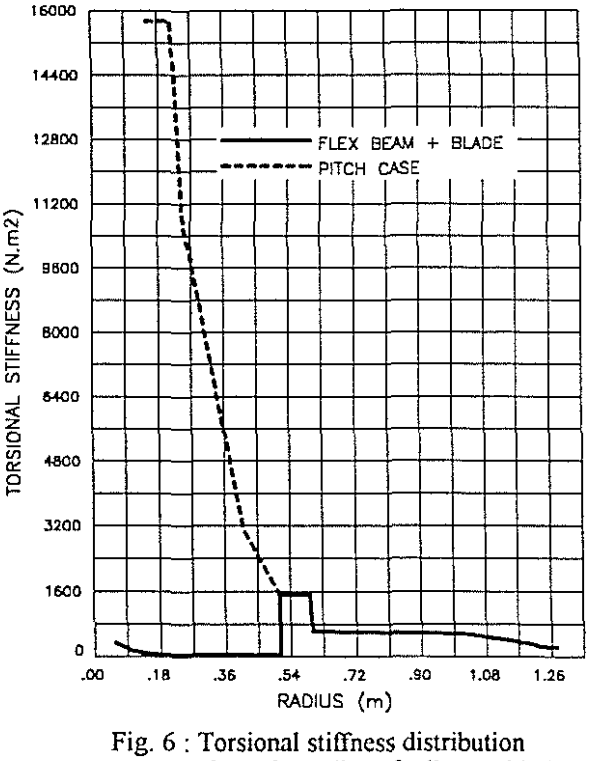

Fig. 6 : Torsional stiffness distribution along the radius of tail rotor blade

The optimum coupled frequencies and mode shapes were calculated through an extensive finite-element analysis. The coupled mode resonance diagram is shown in Fig. 7 along with whirl tower test results.

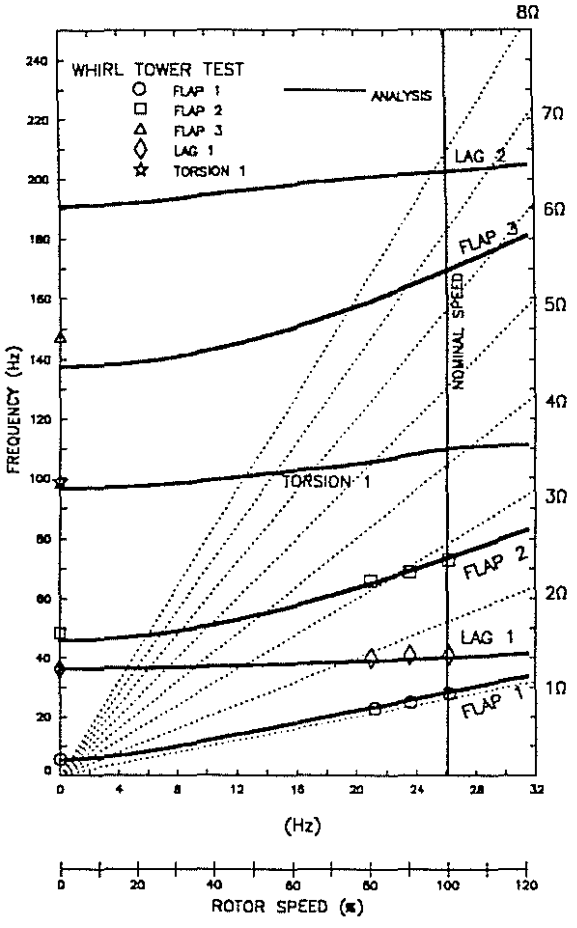

Fig. 7 : Tail Rotor Resonance Diagram

The stiff-in-plane rotor concept is free from aeromechanical stability restrictions (Ref. 1). Flap-lag instabilities have been avoided by suitably placing the flap and lead-lag frequencies. Placement of frequencies to avoid flap-lag instabilities compared with those of other helicopters is shown in Fig. 8 (Ref. 2 & 3).

Avoidance of flutter instability is ensured by the selection of airfoil with adequate aerodynamic torsional damping characteristics and proper placement of the centre of gravity, elastic axis and aerodynamic centre locations.

5. GROUND TESTING

Extensive ground tests were conducted at component level to establish the static and fatigue

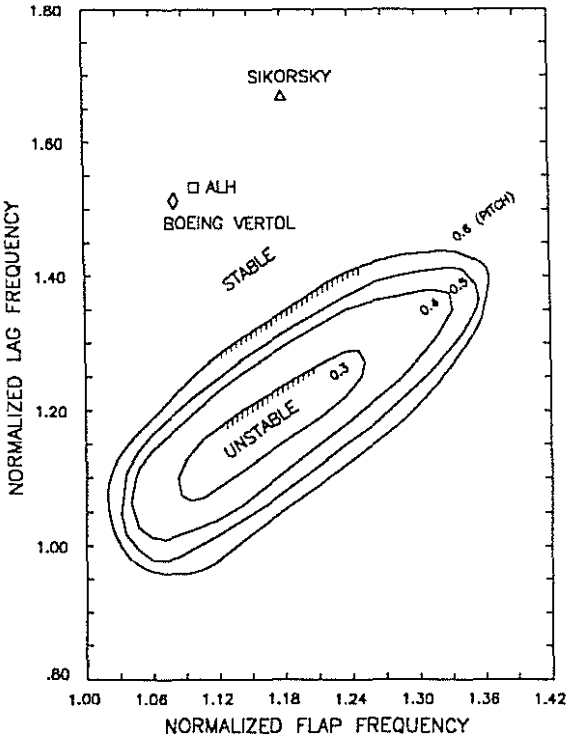

Fig. 8 : Flap-Lag stability boundary

strength capability. Whirl tower tests were carried out to evaluate the dynamic characteristics of the tail rotor system. As a part of endurance runs, tail rotor system was tested over its operating range on Ground Test Vehicle (GTV) which is similar to helicopter but anchored to ground.

5.1 Component Tests

Tests were conducted on the following tail rotor components :

- Tail rotor blade pair
- Hub plates
- Snubber bearing
- Tail rotor shaft
- Pitch horn
- Spider
- Pitch link
- Control tube interface

Static and fatigue tests were conducted on the tail rotor blade pair to establish the capability. In this regard, short blade and long blade tests were conducted simulating the centrifugal, flap and lead-lag forces to create failure in the flexbeam and airfoil area respectively.

Hub test specimen consists of the two titanium lower and upper hub plates, two pair of short blades, a portion of tail rotor shaft and associated fasteners. Centrifugal force on blades were applied through four servo actuators. Flap and lead-lag moment on the blades were created by another four actuators and operated with 90° phase lag to simulate rotating bending on the shaft. Fig. 9 shows the ground test set up for hub assembly test.

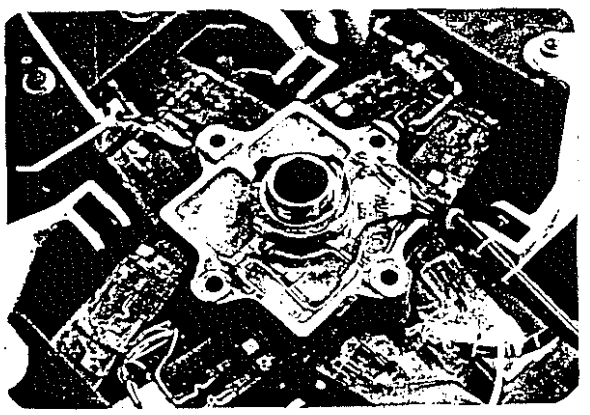

Fig. 9 : Ground test set-up for tail rotor hub assembly test

Stiffness, limit load and fatigue tests were carried out on snubber bearing assembly at various load and motion spectrum.

The tail rotor shaft was subjected to rotating bending test on a special test rig. The shaft was mounted on bearings as in the tail gear box. Constant bending moment was applied to the shaft.

Pitch horn, spider and pitch link were tested on the universal testing machines by designing special fixtures to simulate appropriate loading conditions.

Using the data of static and fatigue tests on the components of tail rotor system, the component allowables in terms of its endurance (α - limit) and low cycle limits (β - limit) were established which helps in defining the weak links of the system. During whirl tower, GTV and flight tests, critical component loads were continuously monitored and recorded for ensuring the structural integrity.

5.2 Whirl Tower Test

A special whirl tower (Fig. 10) test facility has been designed and dynamically tuned so as to run the stiff-in-plane tail rotor over the complete rotational speed range without the tower itself getting into resonance. The precession capability of the whirl tower was used to establish maximum loads and strains under simulated yaw turns. On this whirl tower, ALH tail rotor was tested for the performance, loads, frequencies, aeroelastic stability characteristics over the complete range of rotational speed, collective pitch angles and precession. The rig was also used for making endurance run. The measured frequencies are compared with analysis in resonance diagram, Fig. 7 which indicate good correlation over the operating speed range.

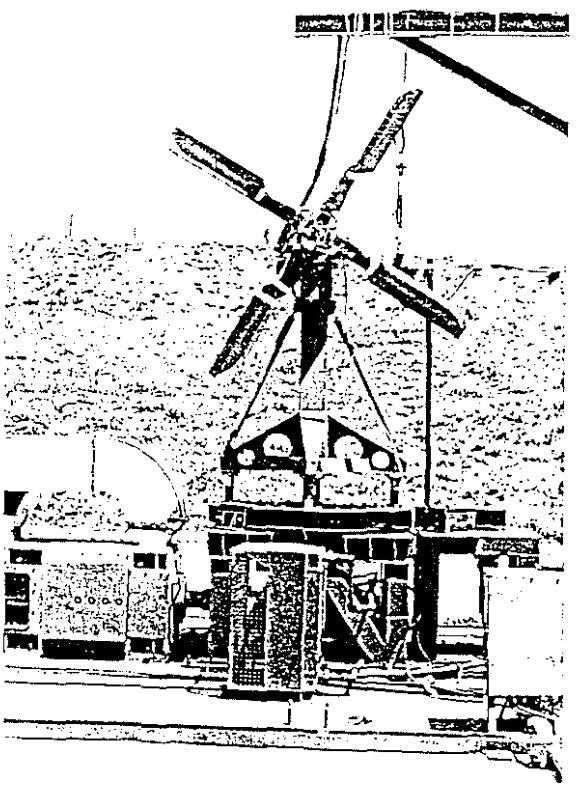

Fig. 10 : Tail Rotor on Whirl Tower

The thrust and power of the tail rotor measured on the whirl tower are shown along with analysis values in Fig. 11 and 12 respectively. Good correlation is observed between analysis and test results.

The measured static flap and lead-lag moments at root of the blade are plotted along with analysis in Fig. 13 and 14 respectively which shows good correlation in lead-lag and significant variation in flap direction at higher pitch angles.

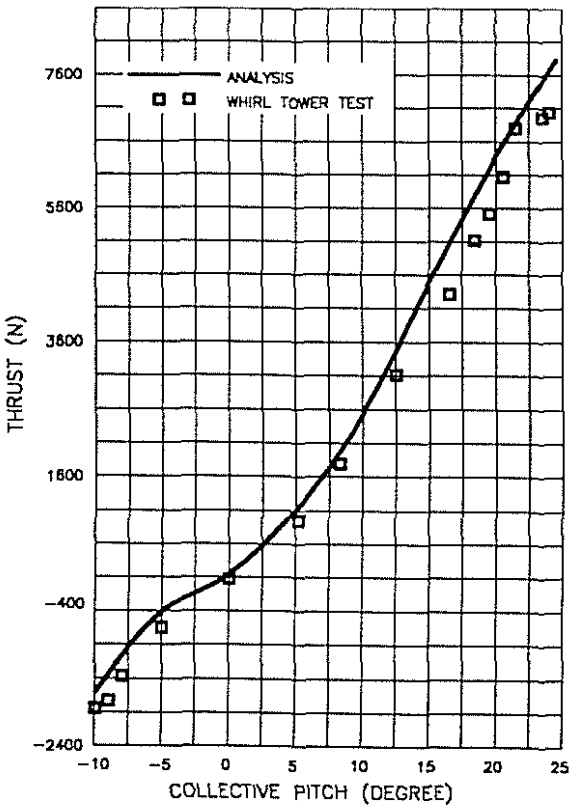

Fig. 11 : Variation of thrust with collective pitch angle

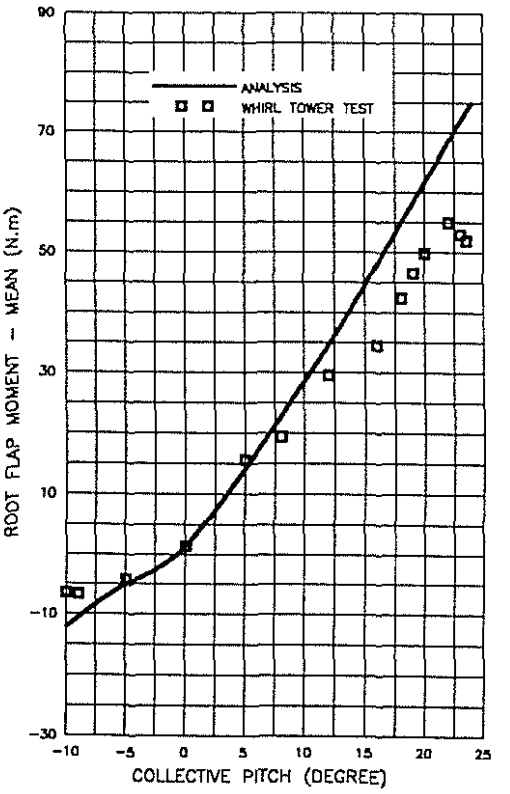

Fig. 13 : Variation of flap moment at root of blade with collective pitch angle

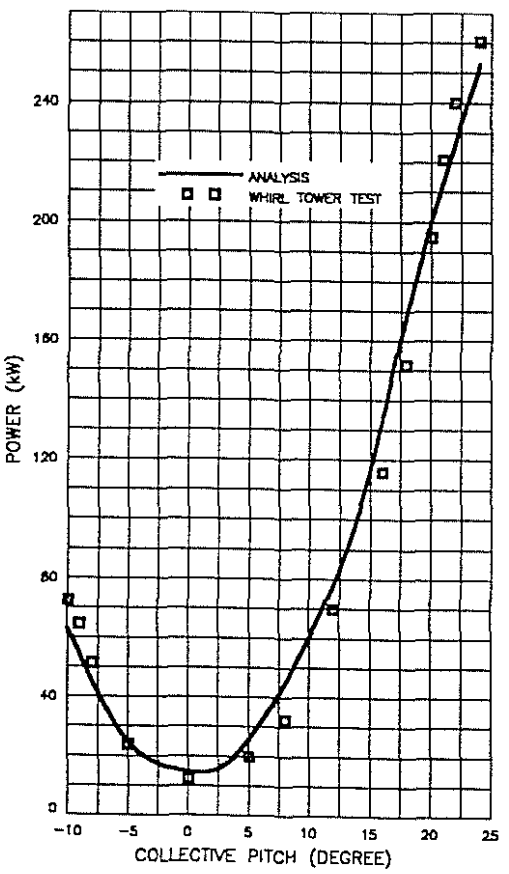

Fig. 12 : Variation of power with collective pitch angle

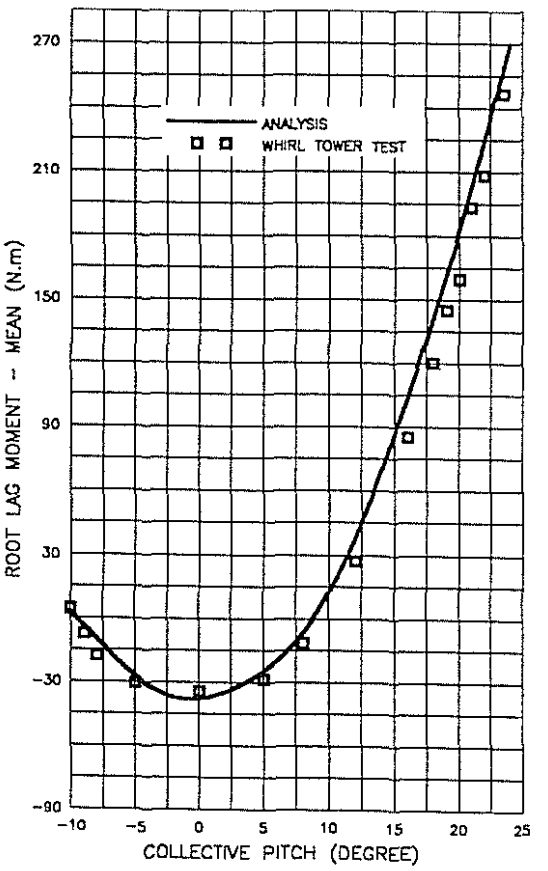

Fig. 14 : Variation of lead-lag moment at root of blade with collective pitch angle

The measured static pitch link forces for various collective pitch angles are higher than the analysis as shown in Fig. 15.

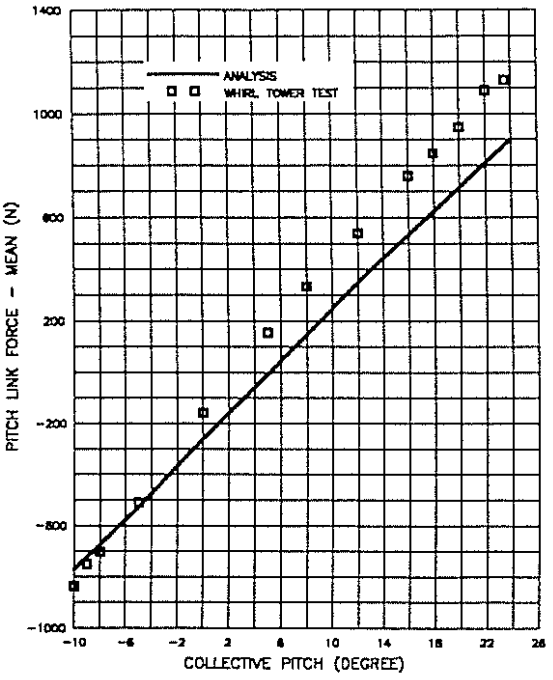

Fig. 15 : Variation of pitch link force with collective pitch angle -tail rotor whirl tower test

The variation of static flap bending moment and pitch link forces with respect to analysis could be due to limitation of theoretical model which considers 1st. flap and lead-lag modes only.

Variations of dynamic flap bending moments measured at root of the blade with precession rate are shown in Fig. 16 for various collective pitch angle setting. Similar trends are seen with lead-lag and pitch link loads.

For damping measurements, the lead-lag rotor mode was excited by shaking the softly supported test rig in the plane of rotation. The natural frequency and the appropriate modal damping were evaluated from the decaying chordwise bending moment after stopping the excitation. The measured frequency and the damping ratio are shown in Fig. 17 and 18 respectively which shows adequacy with respect to inplane damping.

5.3 Ground Test Vehicle

The functional characteristics of tail rotor were tested on GTV for complete range of pedal positions as a part of certification requirements. The tail rotor system has run on GTV nearly 400 hours including

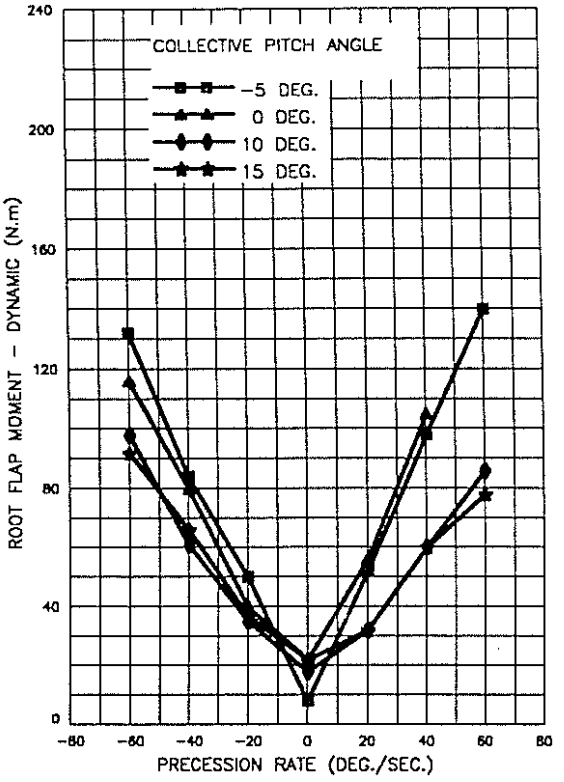

Fig. 16 : Variation of flapping moment at root with precession rate -tail rotor whirl tower test

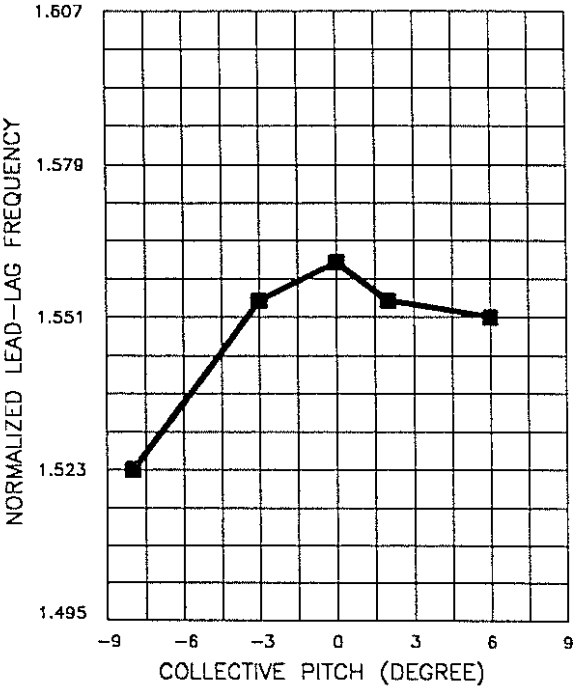

Fig. 17 : Variation of lag frequency with collective pitch-whirl tower test

functional and load runs. The tail rotor assembly was disassembled at specific intervals to observe the conditions of the parts in terms of crack, wear,

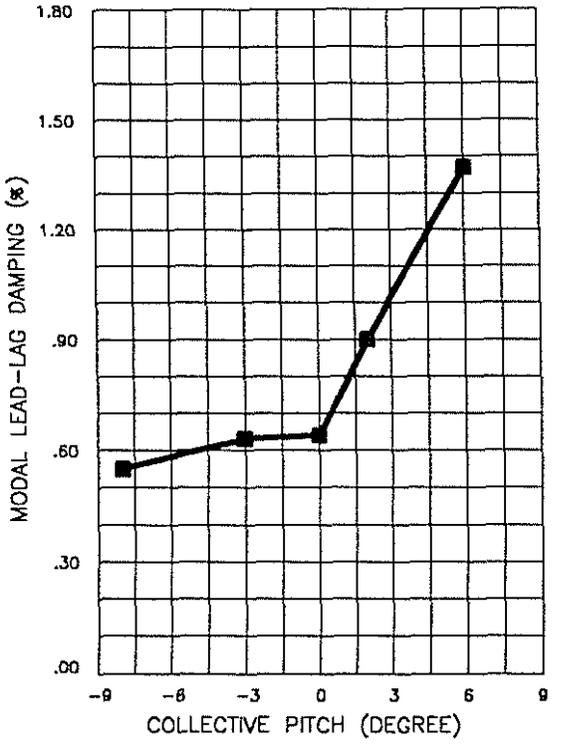

Fig. 18 : Variation of damping with collective pitch angle-whirl tower test

Fig. 19 : Bearingless tail rotor assembled on prototype of ALH

debond etc. The tail rotor system has worked satisfactorily during GTV runs.

6. FLIGHT TEST

The bearingless tail rotor which has been fitted on all the four prototypes (Fig. 19) has undergone flight tests at Bangalore covering the flight envelope. In addition, flights critical to tail rotor systems like sideslips, spot turns and sideward flights have also been done to assess the performance, loads and control margins. As a part of certification, the prototypes have undergone flight tests at sea level, cold (high altitude) and hot weather trials. During these trials, tail rotor system has demonstrated satisfactory performance with respect to loads, vibration level and control margins. The tail rotor fitted on Naval version of ALH has been adequately tested for its low speed handling characteristics during ship deck trials.

Fig. 20 and 21 give the measured dynamic flap and lead-lag bending moments at the flexbeam root with respect to forward speed. The measured loads are within the component capability indicating sufficient fatigue life. Similar trends can be seen on the pitch link and rotor shaft loads as indicated in Fig. 22 and 23.

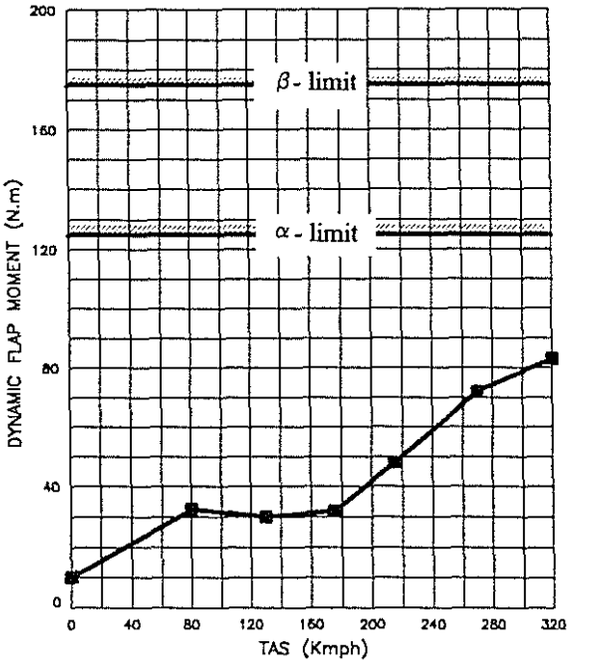

Fig. 20 : Variation of dynamic flap moment with forward speed-flight test

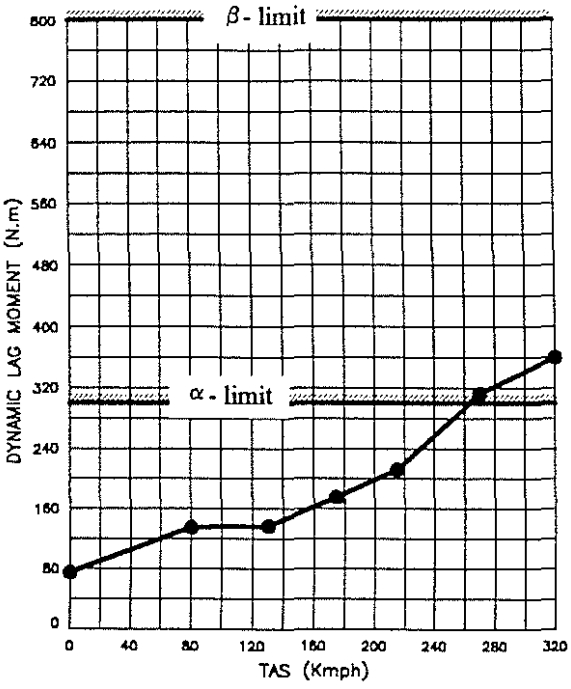

Fig. 21 : Variation of dynamic lag moment with forward speed - flight test

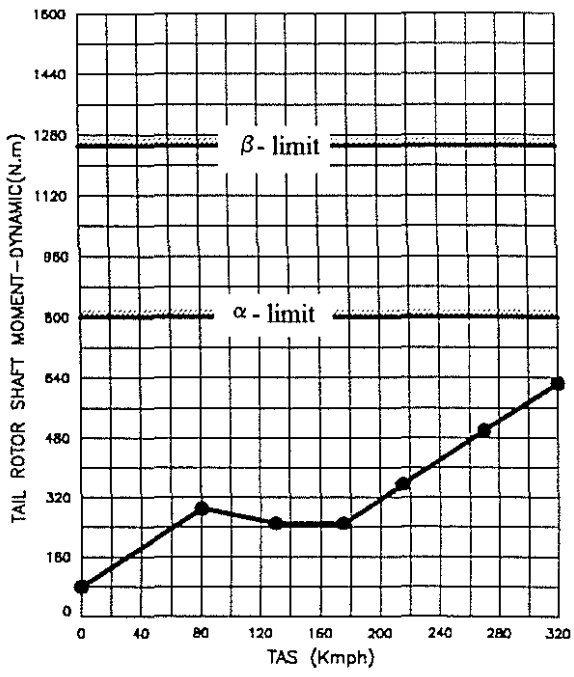

Fig. 23 : Variation of tail rotor shaft moment with forward speed - flight test

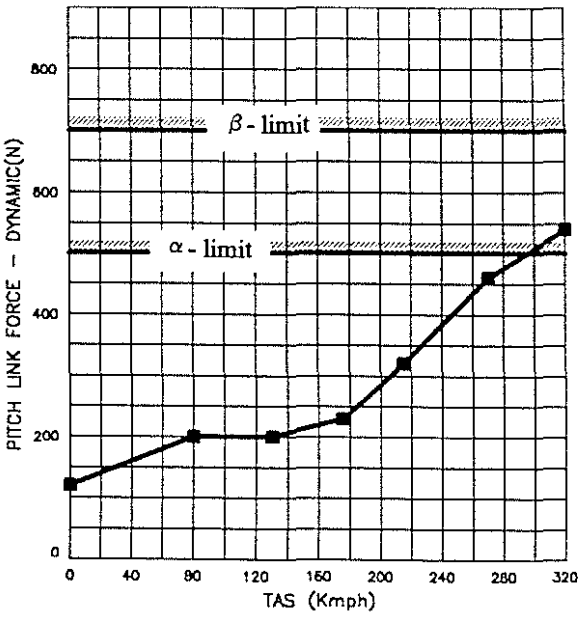

Fig. 22 : Variation of dynamic pitch link force with forward speed - flight test

The pitch link and rotor shaft loads with respect to pedal positions for some of the critical flight conditions are indicated in Fig. 24 and 25 along with the component capability indicating adequacy in design.

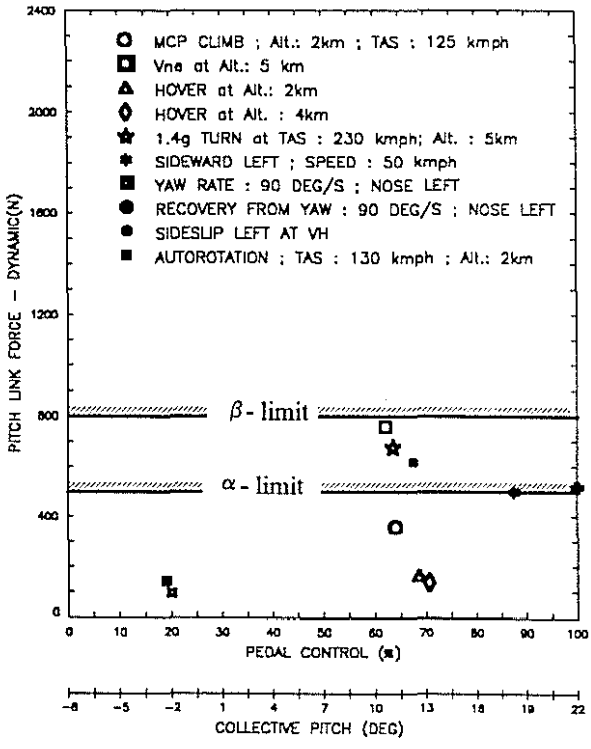

Fig. 24 : Tail rotor pitch link force vs. pedal positions for some critical flights

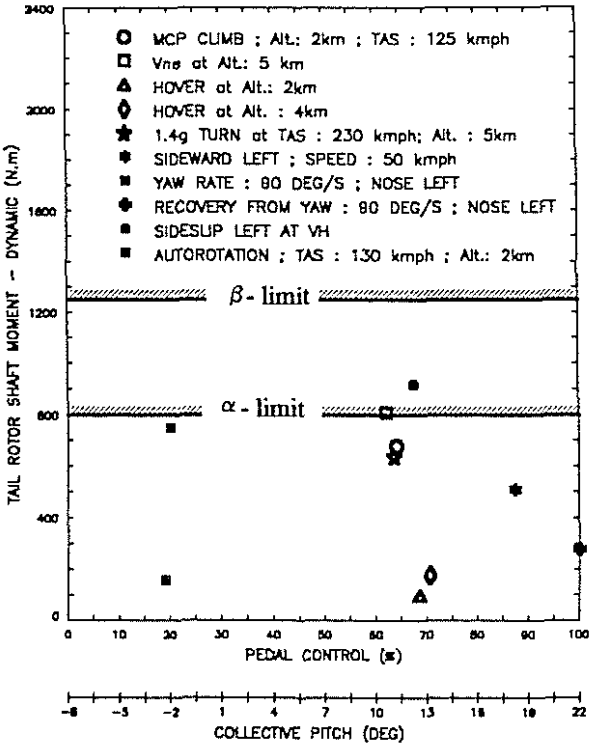

Fig. 25 : Tail rotor shaft moments vs. pedal positions for some critical flights

8. CONCLUSIONS

- dynamic characteristics with respect to frequency placement as measured on whirl tower are on par with analysis
- the measured loads on flexbeam root, pitch link and rotor shaft are within the component capability ensuring good fatigue life
- rotor does not show any aeroelastic instability over the complete flight envelope

9. REFERENCES

1. 'Development of bearingless tail rotors' *by V. Kloppel, H. Huber and B. Enenkel, Messerschmitt-Bolkow-Blohm;* 16th.European Rotorcraft Forum Proceedings, 1990.

2. 'Helicopter Dynamics' by Bramwell

3. 'Helicopter Theory ' by Wayne Johnson